

Supporting Information for

Multifunctional Photo-Crosslinked Polymeric Ionic Hydrogel Films

Hongkun He,^{1,2} Brian Adzima,² Mingjiang Zhong,¹ Saadyah Averick,¹ Richard Koepsel,³ Hironobu Murata,³ Alan Russell,³ David Luebke,² Atsushi Takahara,⁴ Hunaid Nulwala,^{1,2,*} and Krzysztof Matyjaszewski^{1,2,*}

¹ *Center for Macromolecular Engineering, Department of Chemistry, Carnegie Mellon University, 4400 Fifth Avenue, Pittsburgh, Pennsylvania 15213*

² *National Energy Technology Laboratory, Pittsburgh, Pennsylvania 15236*

³ *Institute for Complex Engineered Systems, Carnegie Mellon University, 4400 Fifth Avenue, Pittsburgh, Pennsylvania 15213*

⁴ *Institute for Materials Chemistry and Engineering, Kyushu University
CE11 Ito Campus, 744 Motoooka Nishi-ku, 819-0395, Japan*

*Corresponding author, E-mail: (H. N.) hnulwala@andrew.cmu.edu, (K. M.) km3b@andrew.cmu.edu.

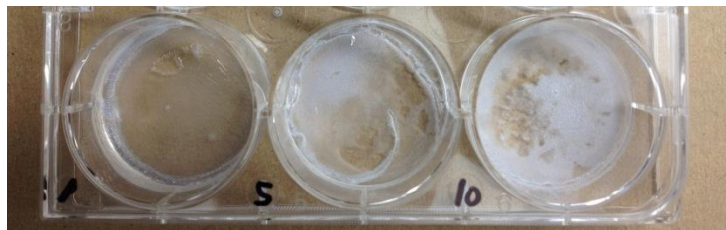


Figure S1. Photos of the products of 100% PEODMA with different concentrations thermally crosslinked at 70 °C (0.5 mL in a round well with diameter of 35 mm). From left to right: without dilution, diluted by 5 and 10 times, respectively.

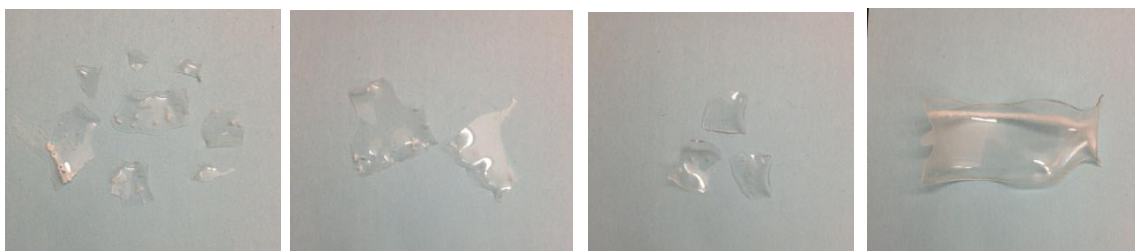


Figure S2. Photos of film samples of the products of 100% PEODMA between two glass slides with aluminum foil spacer of 4, 8, 16, and 32 layers (from left to right) thermally crosslinked at 70 °C.



Figure S3. Photos of film samples of the products of 100% PEODMA between two glass slides with the gap between the slides sealed and aluminum foil as the spacer of 4, 8, 16, and 32 layers (from left to right) thermally crosslinked at 70 °C.

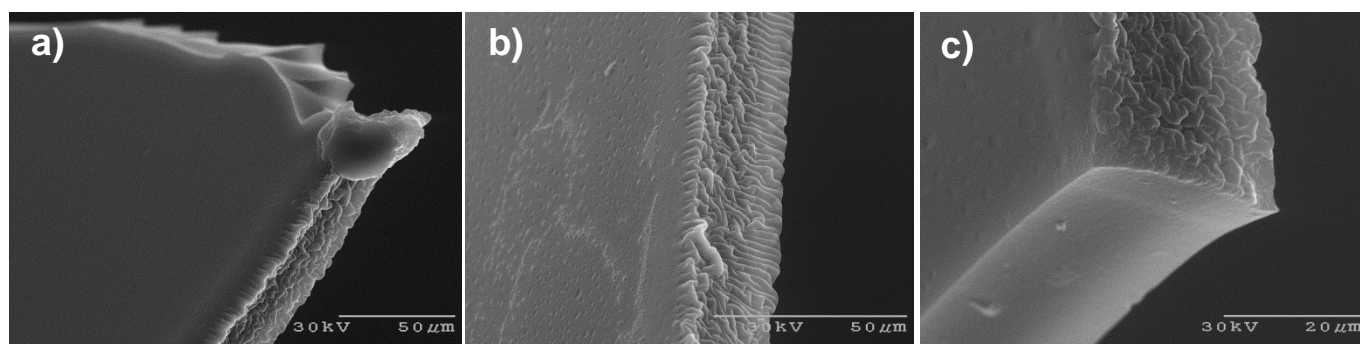


Figure S4. SEM images of cross-section of the VBTMAcI/PEODMA films (20 μm thickness) with different crosslinking degrees: 80% (a), 60% (b), and 20% (c).

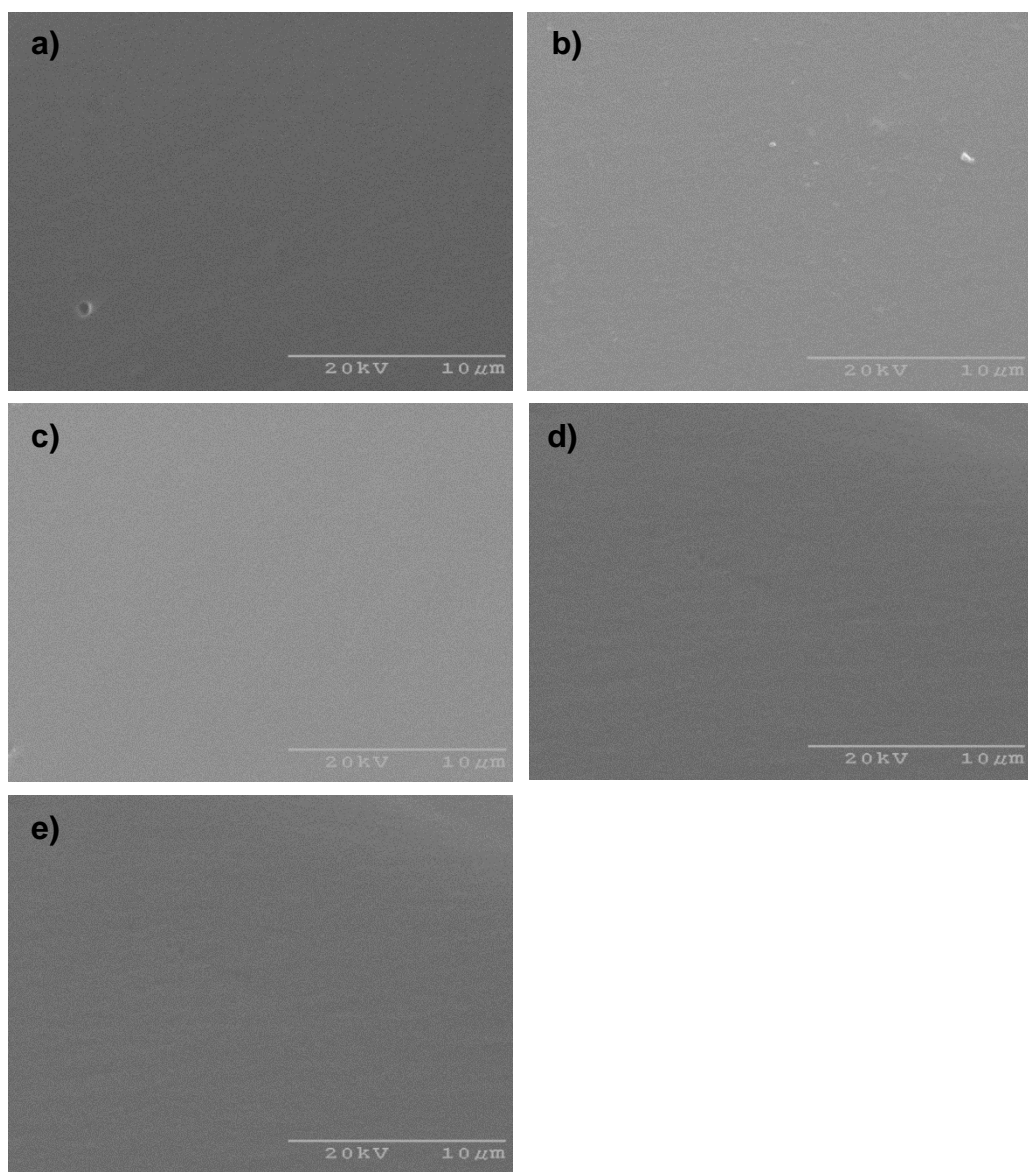


Figure S5. SEM images of the fracture surfaces broken in liquid nitrogen of VBTMACI/PEODMA films (1 mm thickness) with crosslinking degrees of 100% (a), 80% (b), 60% (c), 40% (d), and 20% (e).

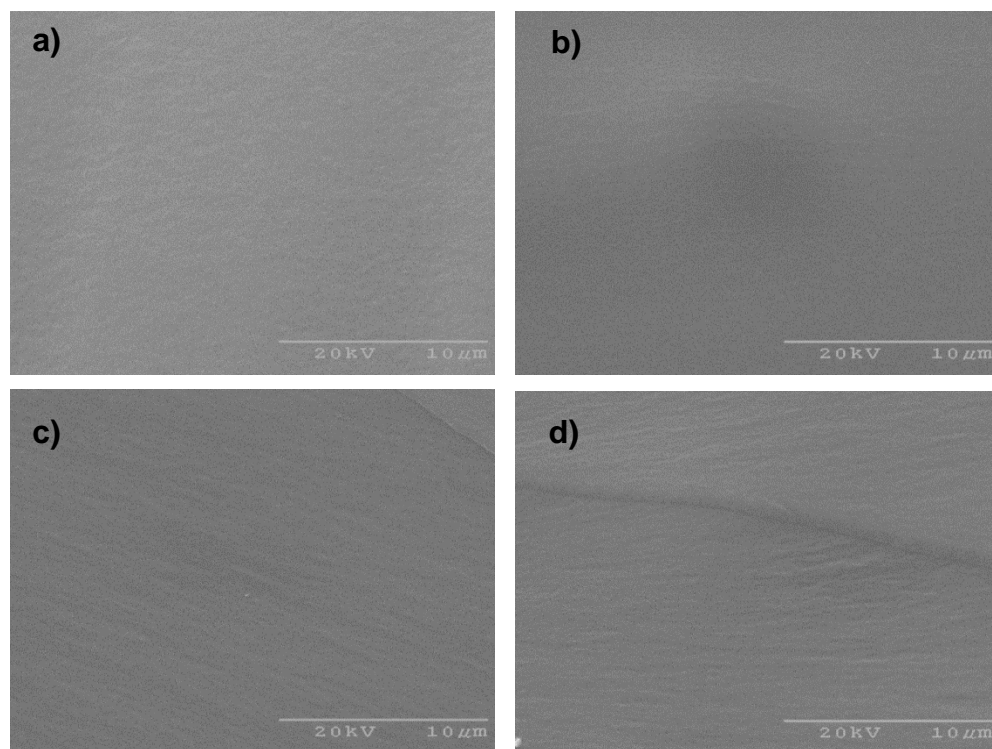
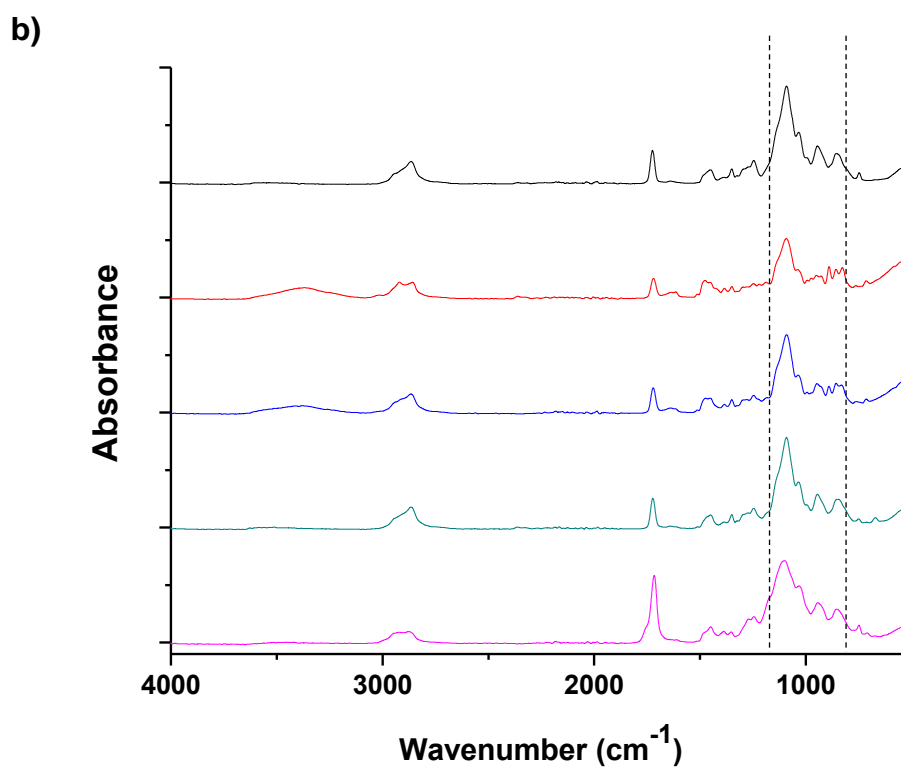
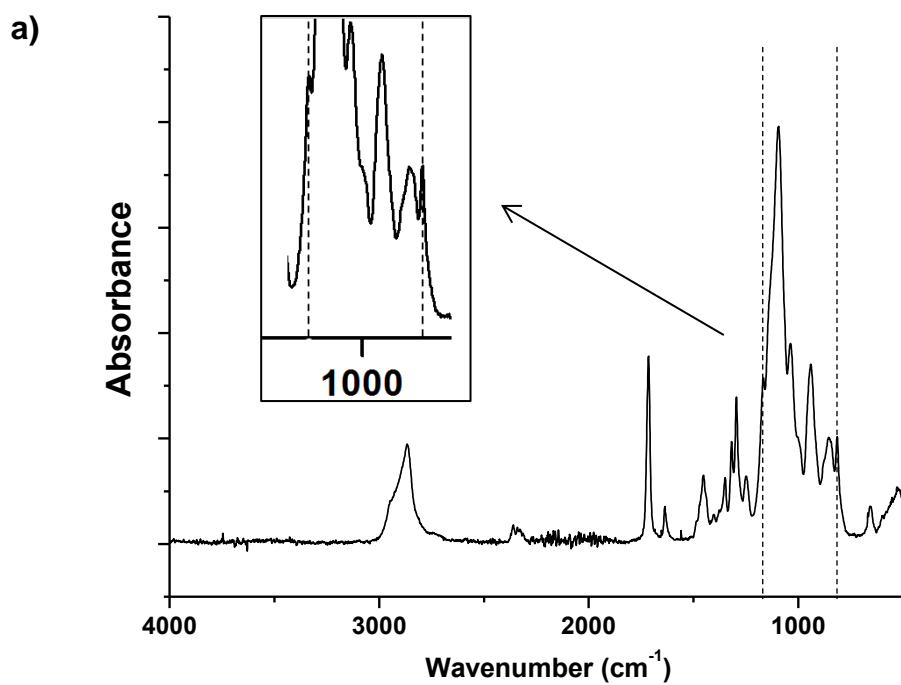


Figure S6. SEM images of the fracture surfaces broken in liquid nitrogen of VBTMAOH/PEODMA films (1 mm thickness) with crosslinking degrees of 80% (a), 60% (b), 40% (c), and 20% (d).



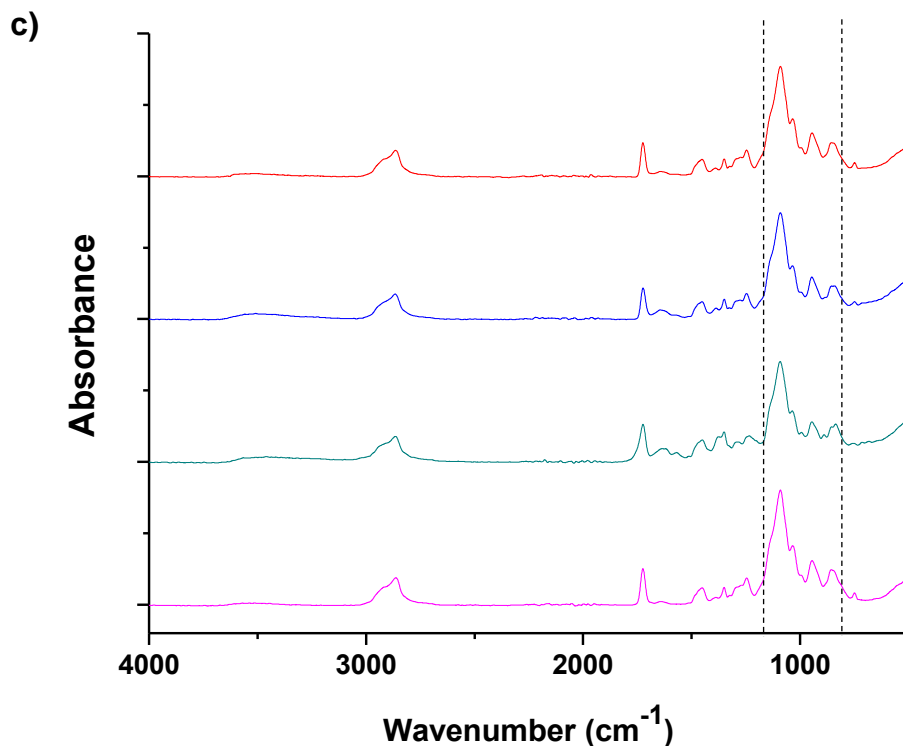


Figure S7. Attenuated total reflection Fourier transform infrared (ATR-FTIR) spectra of (a) PEODMA, (b) VBTMACI-PEODMA films (1 mm thickness) with crosslinking degrees of 100%, 80%, 60%, 40%, and 20% (from top to bottom), and (c) VBTMAOH-PEODMA films (1 mm thickness) with crosslinking degrees of 80%, 60%, 40%, and 20% (from top to bottom). The dash lines indicate the wavenumbers corresponding to vinyl peaks at 814 and 1170 cm⁻¹.

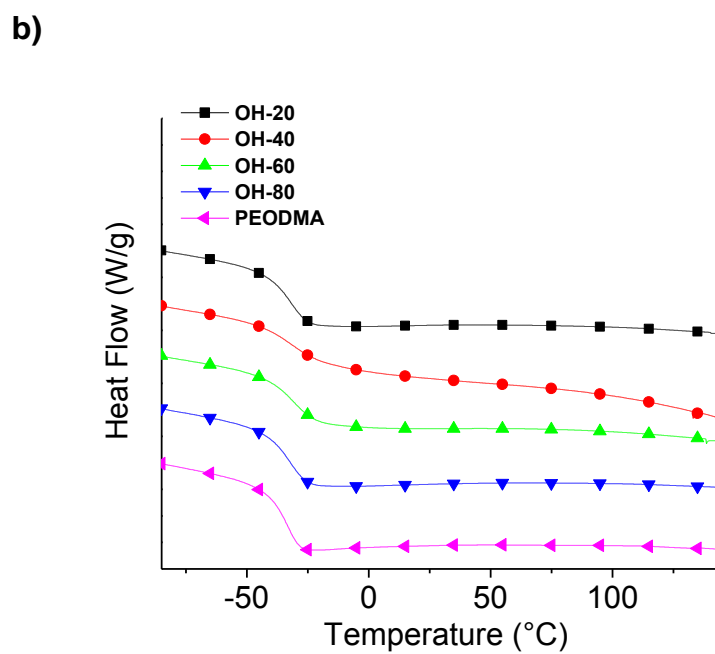
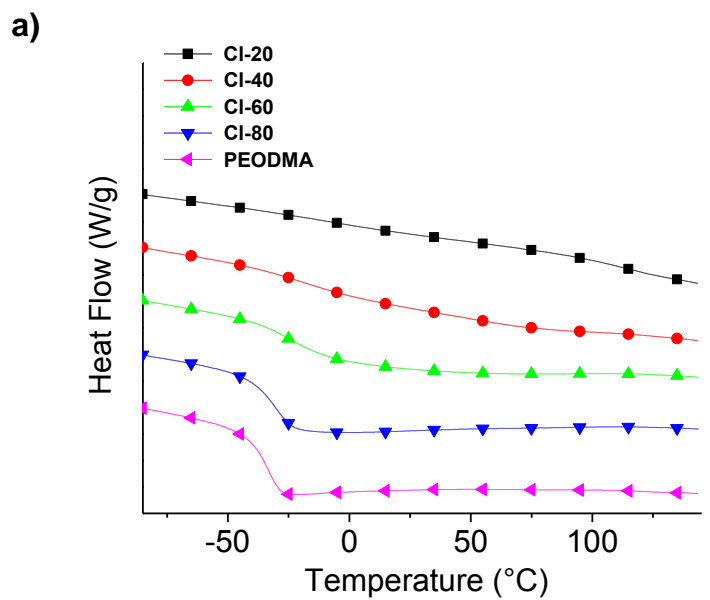


Figure S8. DSC curves of VBTMACl-PEODMA (a) and VBTMAOH-PEODMA (b) films for the third heating cycle.

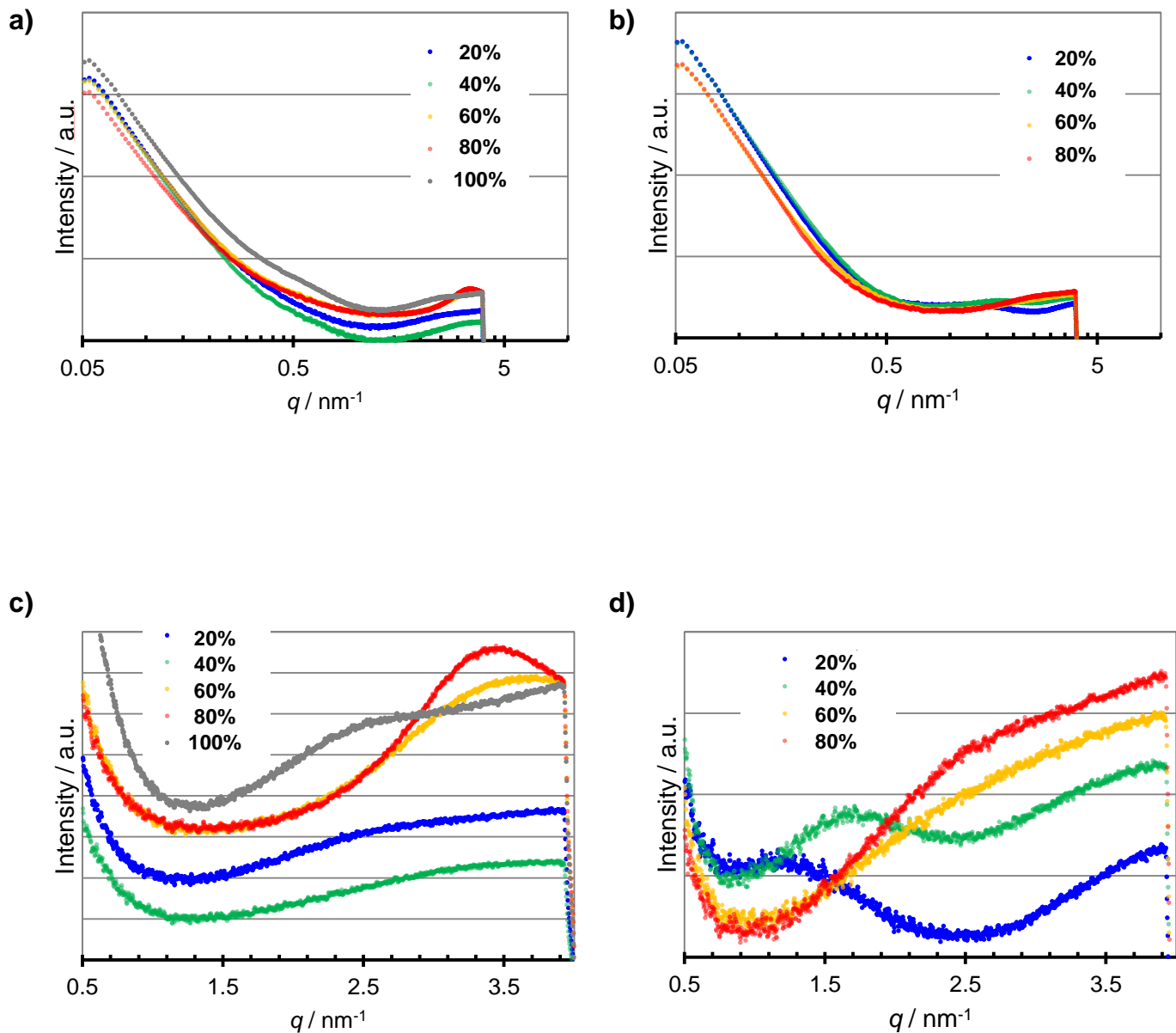
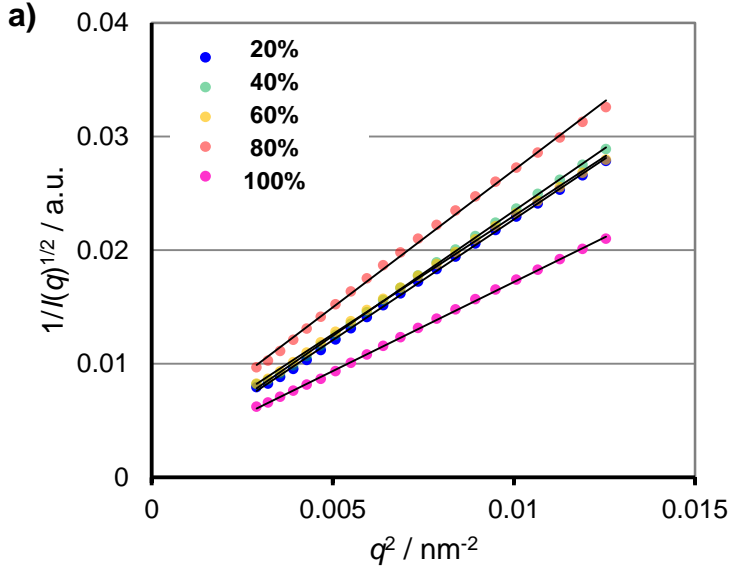
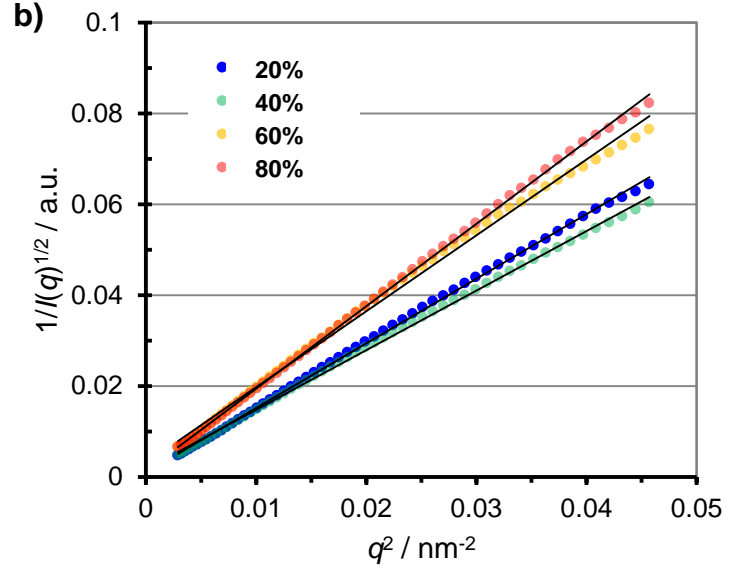


Figure S9. SAXS intensity profiles for VBTMACI-PEODMA (a,c) and VBTMAOH-PEODMA (b,d) films. Magnified views in the q -range from 0.5 to 3.8nm^{-1} of (a,b) are shown in (c,d). The norm value of the scattering vector, q in the horizontal axis, is defined as $4\pi\sin\theta/\lambda$, where θ is Bragg angle (the half value of scattering angle) and λ is the x-ray wavelength.



	Intercept	Slope	ξ / nm
20%	0.001431	2.125	38.5
40%	0.001444	2.199	39.0
60%	0.002165	2.084	31.0
80%	0.002876	2.415	29.0
100%	0.001499	1.569	32.4



	Intercept	Slope	ξ / nm
20%	0.000887	1.423	40.1
40%	0.001632	1.312	28.4
60%	0.003016	1.672	23.5
80%	0.001267	1.814	37.8

Figure S10. Debye plots for VBTMACI-PEODMA (a,c) and VBTMAOH-PEODMA (b,d) films. The correlation length ξ estimated by above plots are shown in the below tables. Debye-Bueche equation (eq. 1) for a random two-phase system was used to estimate the correlation length ξ , a measure of the spatial size of fluctuations.¹⁻³

$$I(q) = \frac{I(0)}{\left(1 + \xi^2 q^2\right)^2} \Rightarrow \frac{1}{\sqrt{I(q)}} = \frac{1}{\sqrt{I(0)}} + \frac{\xi^2}{\sqrt{I(0)}} q^2 \quad (\text{eq. 1})$$

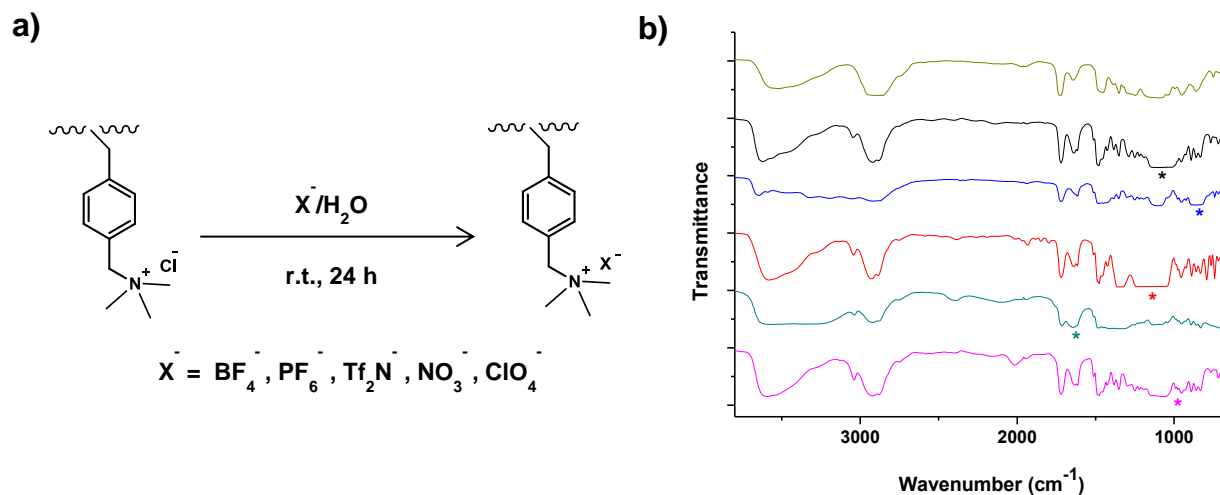


Figure S11. (a) Ion-exchange of the anions in the VBTMACI-PEODMA films. (b) FTIR spectra of VBTMACI-PEODMA films (20% crosslinking, 20 μm thickness) without ion exchange, and ion-exchanged with NaBF_4 , NH_4PF_6 , LiTf_2N , NaNO_3 , and NaClO_4 (from top to bottom). The asterisks indicate the characteristic IR absorption bands of BF_4^- , PF_6^- , Tf_2N^- , NO_3^- , and ClO_4^- , respectively.

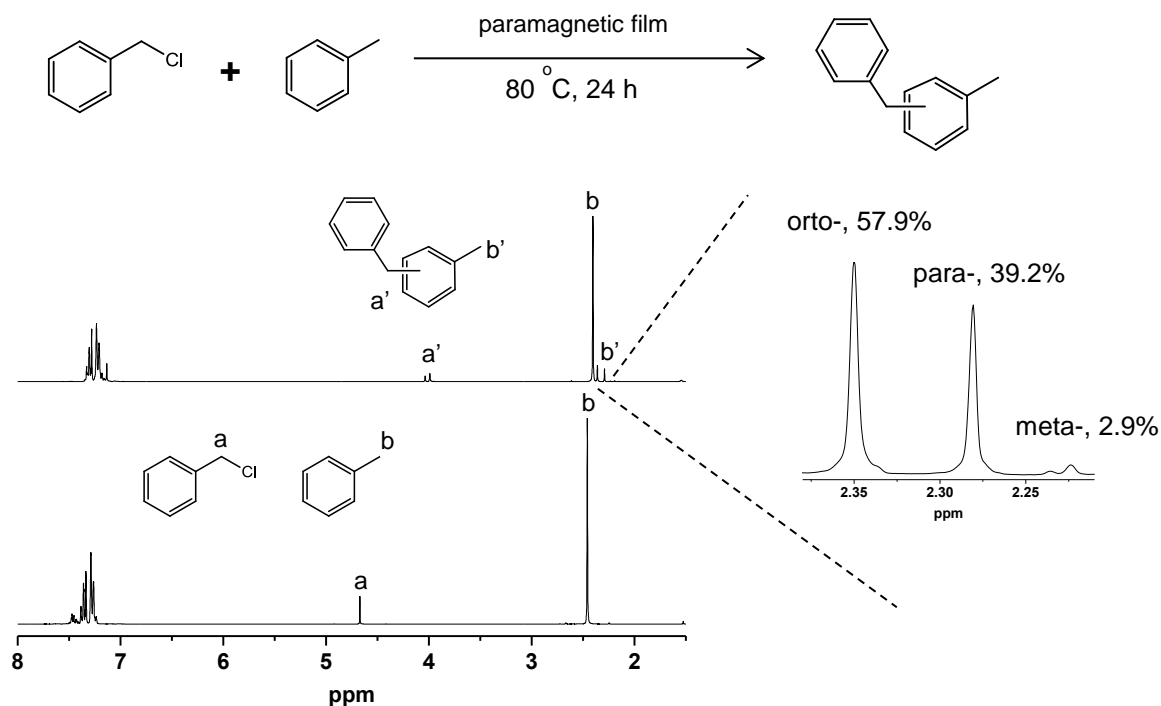


Figure S12. ^1H NMR analysis of the reaction of toluene and benzyl chloride in the presence of paramagnetic film.

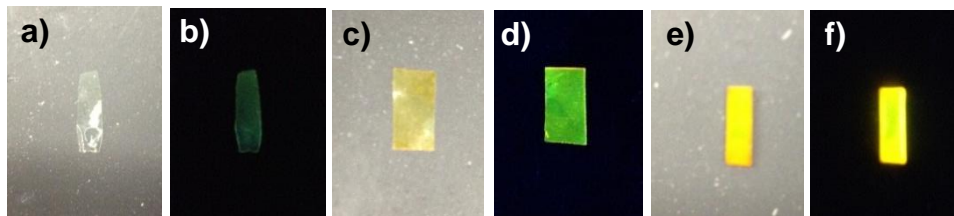


Figure S13. Photos of films loaded with fluorescein under white light (a, c, e) and 365 nm UV light (b, d, f): (a, b) VBTMACI-PEODMA film (100% crosslinking, 20 μm thickness), (c, d) VBTMACI-PEODMA film (20% crosslinking, 20 μm thickness), and (e, f) VBTMACI-PEODMA film (20% crosslinking, 1 mm thickness).

The films were soaked in an aqueous solution of fluorescein for one day and dried at ambient conditions. As shown in Figure S13, after loading with fluorescent dyes of fluorescein, the color of VBTMACI-PEODMA films (20% crosslinking, 20 μm thickness) in white light changed from nearly transparent to yellow, and showed obvious fluorescence under UV light. In contrast, VBTMACI-PEODMA film (100% crosslinking, 20 μm thickness) with no quaternary ammonium chloride groups did not show strong fluorescence. In addition, when the much thicker VBTMACI-PEODMA film (20% crosslinking, 1 mm thickness) was used, the fluorescence became much stronger due to the presence of more quaternary ammonium chloride groups and thus higher content of fluorescent dyes. The films in Figure S13 were scanned with a laser scanner to quantify the fluorescence intensities (Figure S14).

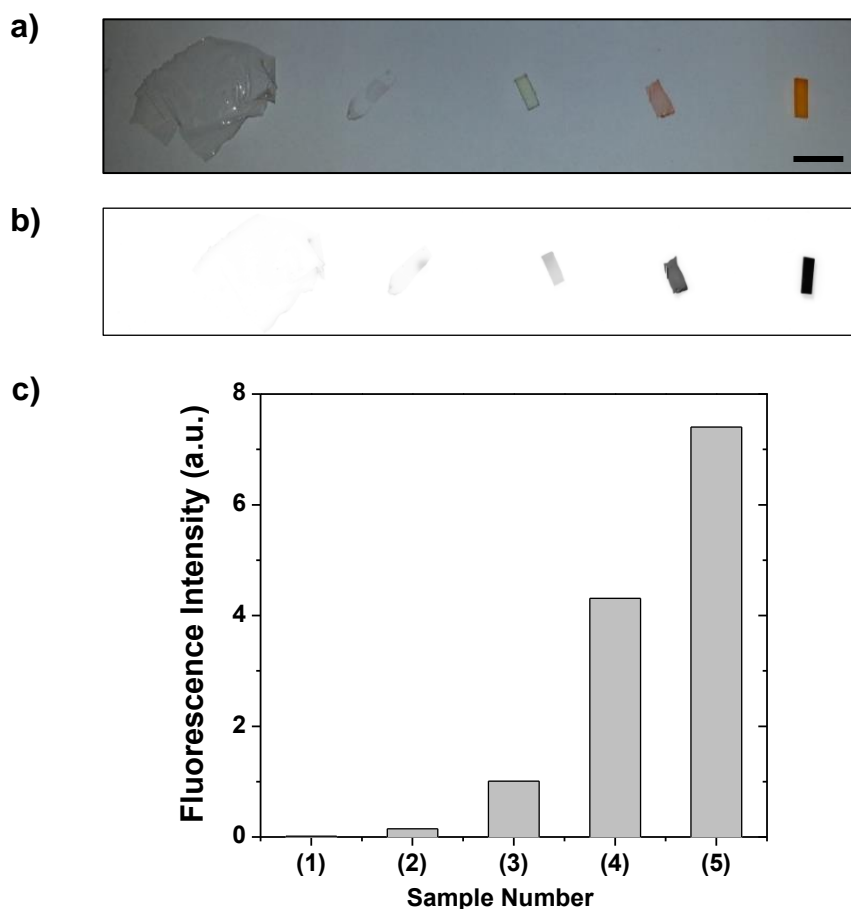


Figure S14. Photos of photo-crosslinked polymeric ionic films (a) under room light (scale bar: 1 cm) and (b) scanned with a GE Typhoon FLA 9000 scanner under 473 nm UV light rendered with gray. (c) Fluorescence intensity of the films measured by a GE Typhoon FLA 9000 scanner. From left to right: (i) control sample of VBTMACI-PEODMA film with no loading of fluorescein (100% crosslinking, 20 μ m thickness), (ii) VBTMACI-PEODMA film (100% crosslinking, 20 μ m thickness), (iii) VBTMACI-PEODMA film (100% crosslinking, 1 mm thickness), (iv) VBTMACI-PEODMA film (20% crosslinking, 20 μ m thickness), and (v) VBTMACI-PEODMA film (20% crosslinking, 1 mm thickness).

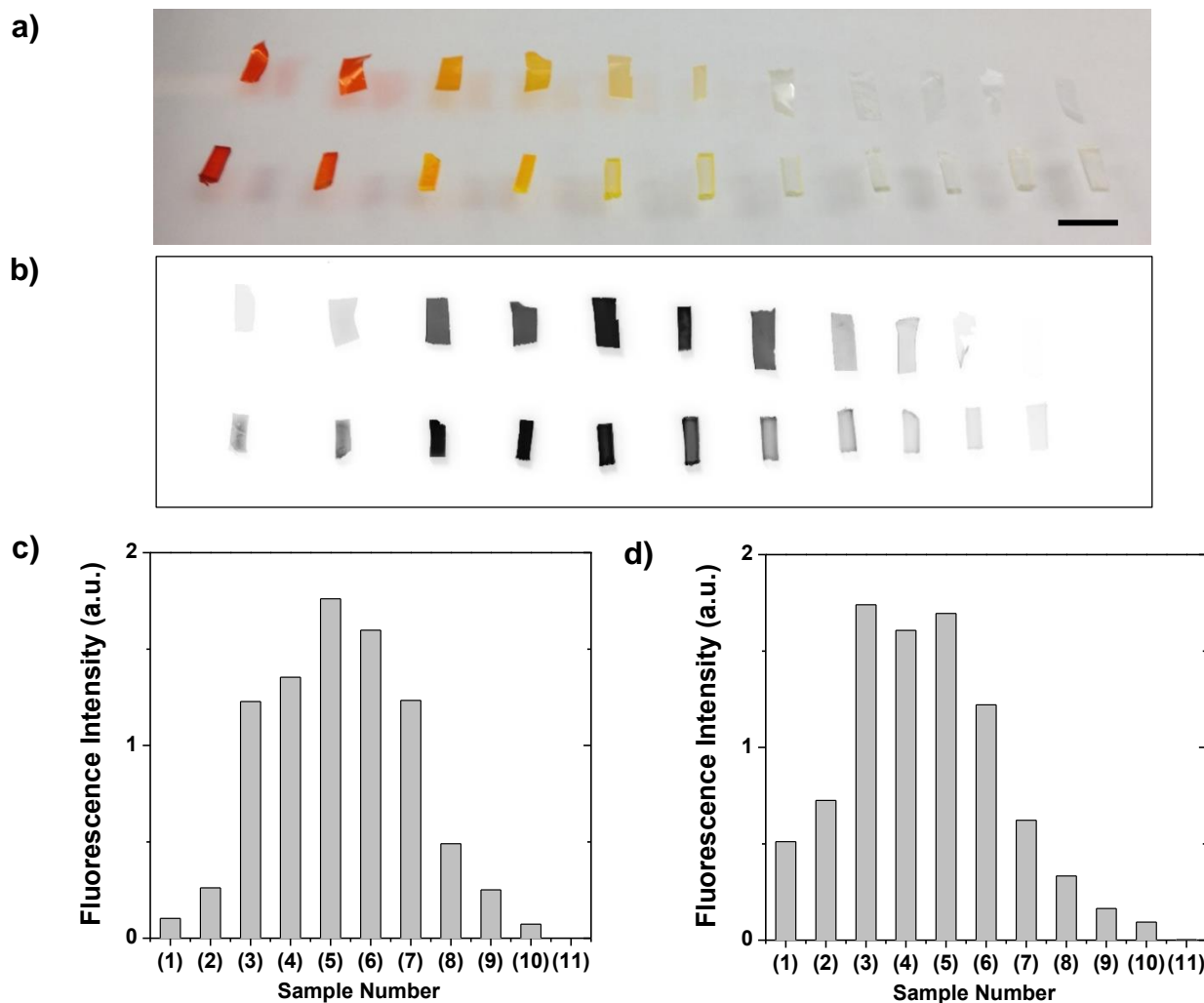


Figure S15. Photos of photo-crosslinked polymeric ionic films (ca. 7 mm \times 3 mm rectangle) under room light (a) and scanned with a GE Typhoon FLA 9000 scanner under 473 nm UV light rendered with gray (b) (scale bar: 1 cm), and the fluorescence intensity of the films measured by a GE Typhoon FLA 9000 scanner (c,d). The upper row in (a) and (b), and (c): VBTMACI-PEODMA films (20% crosslinking, 20 μ m thickness); the lower row in (a) and (b), and (d): VBTMACI-PEODMA films (20% crosslinking, 1 mm thickness). From left to right: the concentrations of the pristine aqueous solutions of fluorescein sodium are (1) 1.0, (2) 0.5, (3) 0.1, (4) 0.05, (5) 0.01, (6) 0.005, (7) 0.001, (8) 0.0005, (9) 0.0001, (10) 0.00005, and (11) 0 mg/mL, respectively.

The films in Figure 8 were then taken out from the solution and scanned with a laser scanner to quantify the fluorescence intensities (Figure S10). Their colors were ranked from the darkest to the

lightest when the concentrations of the fluorescent solution they have been soaked in decreased from 1.0 mg/mL to 0 mg/mL, as observed by naked eyes. However, when they were scanned under 473 nm UV light, their fluorescence intensities did not show a linear correlation with the concentrations. For several samples with the highest concentrations, they showed decreased fluorescence intensities, which was caused by the self-quenching at high concentration.

Reference

1. Debye, P.; Anderson, H. R.; Brumberger, H. *J. Appl. Phys.* **1957**, 28, 679-683.
2. Shiwaku, T.; Nakai, A.; Hasegawa, H.; Hashimoto, T. *Macromolecules* **1990**, 23, 1590-1599.
3. Pogodina, N. V.; Siddiquee, S. K.; van Egmond, J. W.; Winter, H. H. *Macromolecules* **1999**, 32, 1167-1174.